ISSN: 0067-2904

Investigation of Nanostructured and Gas Sensing of Tin Dioxide (Sno_2) Films Prepared by Oxidation of Sn

Mazin H. Hasan[1], Fuad T. Ibrahim[2]*, Ahmed Naji Abd[3]
[1]University of Anbar, College of Science, Physics department, Anbar, Iraq
[2]Baghdad University, College of Science, Physics Department, Baghdad, Iraq
[3]University of Al-Mustansiriyah, College of Science, Baghdad, Iraq

Abstract

Nanostructured tin dioxide (SnO_2) thin films were prepared by thermal oxidation of Sn, which were ground and embedded in methanol then it was deposited on a glass substrate utilizing casting method. The deposited films were examined for their morphology, and crystal structure by transmission electron microscopy (TEM) scanning electron microscopy (SEM), and X-ray diffraction (XRD) technique. In most cases, it was found that SnO_2 thin films had a tetragonal phase, predominantly grown on preferred (110) and (200) planes. The deposited thin films have grain size was about 82 nm. The sensing properties of SnO_2against NO_2 gas were studied as a function of working temperature and time under optimal condition. The sensitivity, response time and recovery time were calculated with different operating temperatures.

Keywords: Tin oxide, Structural properties, Optical properties, TEM, SEM, gas sensing.

فحص التراكيب النانوية زالتحسسية الغازية لاغشية ثاني اوكسيد القصدير المحضرة بالاكسدة الحرارية للقصدير

مازن حامد حسن[1]، فؤاد طارق ابراهيم[2*]، احمد ناجي عبد[3]
[1]قسم الفيزياء، كلية العلوم، جامعة الانبار، الانبار، العراق
[2]قسم الفيزياء، كلية العلوم، جامعة بغداد، بغداد، العراق
[3]قسم الفيزياء، كلية العلوم، الجامعة المستنصرية، بغداد، العراق

الخلاصة

تم تحضير اغشية رقيقة من ثاني أكسيد القصدير النانوي (SnO2) بواسطة الأكسدة الحرارية للقصدير، حيث تم طحنها ودمجها مع الميثانول ثم تم ترسبها على الواح زجاجية باستخدام طريقة الصب. تم فحص البنية التكيبة وهيكل بلوري الاغشية المرسبة بواسطة مجهري الإلكتروني النافذ (TEM) مجهر إلكتروني ماسح (SEM) ، وتقنية حيود الأشعة السينية (XRD). في معظم الحالات ، وجد أن الأغشية الرقيقة لثاني اوكسيد القصدير لديها طور الرباعي ، الذي يظهر في الغالب على المستويين المفضلتين (110) و (200). وكذلك وجد ان حجم الحبيبات الرقيقة حوالي 82 نانومتر. تمت دراسة خصائص التحسسية لثاني اوكسيد القصدير لغاز ثاني اوكسيد الناتروجين (NO2) كدالة لدرجة حرارة وتغيرالزمن في ظل أفضل الظروف. تم حساب الحساسية وزمن الاستجابة وزمن الاسترداد مع درجات حرارة التشغيل المختلفة.

*Email: fuadtariq2002@yahoo.com

1. Introduction

In recent years, attempts have been made for searching non-toxic, low cost, effective new materials which are tailor-made for that purpose. There has been exponential growth in research activities dealing with nanoparticles for humidity sensing applications [1]. This was because of high demands for simple, responsive and stable electronic sensors, which is suitable for environmental monitoring in industries, air pollution control, safety at mining sites and firefighting. Several alternative semiconductors are known to have appropriate properties such as absorption coefficient, band gap energy and diffusion lengths of charge carriers, but didn't lead to higher efficiencies, yet. Hence, it is interesting to sophisticate a new type, cheap and higher yielding inorganic solar cells [2]. Semiconductor nanomaterials have a higher interest in gas sensing application due to their low-cost, high surface to volume ratios, favorable sensitivity, and structural stability [3, 4]. A wide bandgap semiconductor with ~4 eV has been globally examined for diverse applications such as supercapacitor [5], lithium ion batteries [6], chemical sensing, solar cells, electrochromic applications [7] and solar harvesting [8]. Tin dioxide (SnO_2) thin films had unique properties such as, optical transparency, high electrical conductivity, relatively high exciton binding energy which is around 130 meV, direct wide band gap, small exciton Bohr radius, high infrared reflectivity, high mobility of electrons and low cost materials [9]. Stannic oxide has been used in many applications including, gas sensors, dye sensitized solar cell photovoltaic, liquid crystal displays, organic light emitting devices and transparent electrodes [10]. Various techniques were utilized to prepare SnO_2 thin films such as thermal evaporation, chemical vapor deposition, rf magnetron sputtering, pulsed laser deposition and spray pyrolysis [11]. In the present work, we had tried to estimate the topography and morphology of SnO_2 utilizing (AFM), (SEM), (TEM) and X-ray diffraction (XRD) techniques in order to ensure a better understanding of these thin films. Deposition using drop casting method of Sn films which were oxidized at 300 ^oC by the inside electric oven.

2. Experimental part

A two gram of tin powder was immersed in absolute 100 ml of methanol for 12h to get colloidal of Sn, then drop casting technique was employed to deposit Sn onto a glass substrate (at 300 ^oC oxidation temperature in oven) by taking a solution using a pipette and putting 5 drops onto a glass substrate, which were first cleaned with a dilute solution of purifier to remove the impurities and organic materials on the surface of the slides. It should be mentioned that several samples were prepared at different conditions, however only most uniform samples were adopted in the present work.

3. Results and discussion

Sharp diffraction peaks belong to well crystalline films, are shown in Figure-1. SnO_2 samples being tetragonal polycrystalline with major peaks appears at $2\theta = 26.65^o$, $33.93^{o,}$ 37.96^o, 51.86^o, 55.34^o, 62.62^o and 79.59^o. These values were in excellent agreement with the standard JCPDS data (Card No. 88-0287). Major peaks were utilized to calculate the average crystallite size(D) introduced by Scherrer equation which can be written as:[12]:

$$D = \frac{0.94\,\lambda}{\beta \cos(\theta)} \quad (1)$$

Where λ is the CuKα wavelength (λ= 0.1542 nm), θ is the diffraction angle, and β is the full width at half maximum. The microstrain (ε) and the dislocation density (σ) calculated by using the relations in equation (3) [13], see Table-1: There is a correlation between the increased value of crystallite size and the decreased value of dislocation density which refer to higher crystallization, where these results have a good agreement with Pinheiro et al.[14].

$$\sigma = \frac{1}{D^2} \quad (2)$$

The microstrain and the average crystallite size (D_{av}) can be obtained by Williamson- Hall relation [15].

$$\beta\, cos\theta_B = \frac{0.94\,\lambda}{D_{av}} + 4\varepsilon\, sin\theta_B \quad (3)$$

Where λ =0.154 nm and θ_B is Bragg angle. From Figure-2 the average crystallite size and the microstrain can be estimated from the intercept and slope respectively. Their values were found to be 21 nm and -2.03 x 10^{-3} for the average crystallite size and microstrain respectively.

Table 1- X-Ray characterization of SnO_2 thin films

2 θ (deg)	*FWHM (deg)*	*(hkl) Planes*	*Crystallite size (nm)*	*Dislocation density x10^{14} (lines/m^{2})*
26.65	0.300	(110)	27.07	13.64624
33.93	0.270	(101)	30.60	10.67573
37.96	0.200	(200)	41.79	5.724181
51.86	0.180	(211)	48.85	4.189008
55.43	0.148	(220)	60.37	2.743164
62.62	0.164	(310)	56.48	3.13472
79.59	0.157	(321)	65.68	2.317459

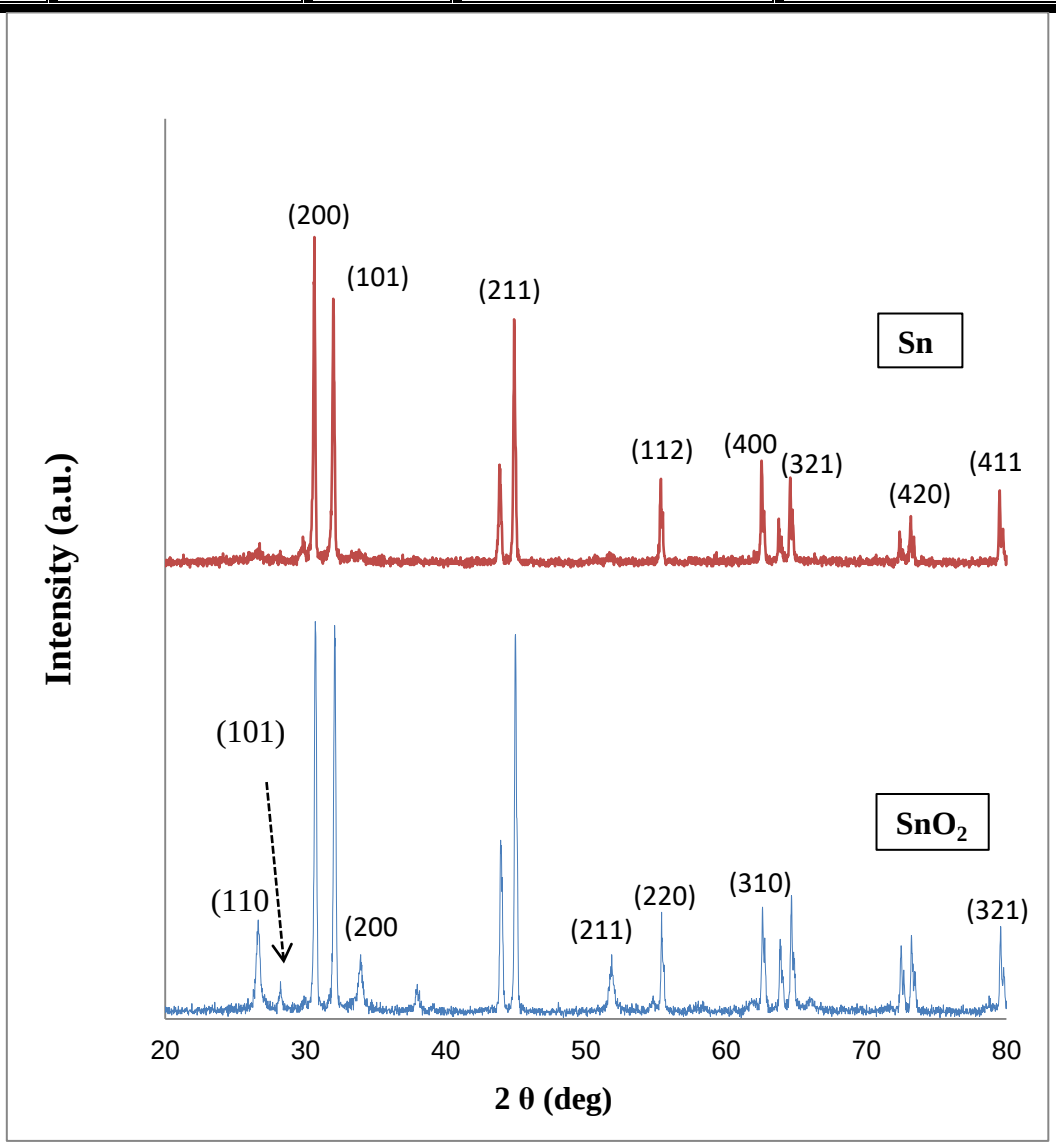

Figure1-XRD patterns of SnO_2 and Sn thin films.

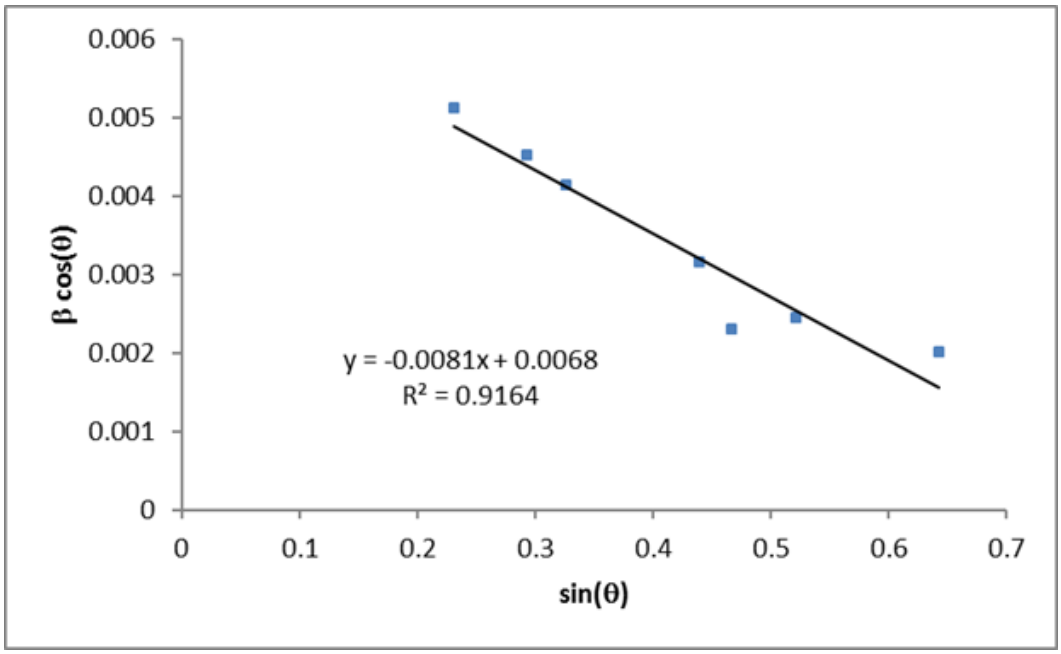

Figure 2-Williamson- Hall plots of as-synthesized SnO_2

Figure-3 shows SEM image with 50 kx magnifications for SnO_2 thin film at 300 ^{O}C oxidation temperatures. SEM image had confirmed that these particles had different morphologies. It can be noticed from the Figure-3, that the particles contained many small asymmetric nanoparticles with agglomeration. Also, the SEM image of SnO_2 thin film had different grain sizes, which were ranged from about 50 nm to 500 nm where some of them were of a cubic shape.

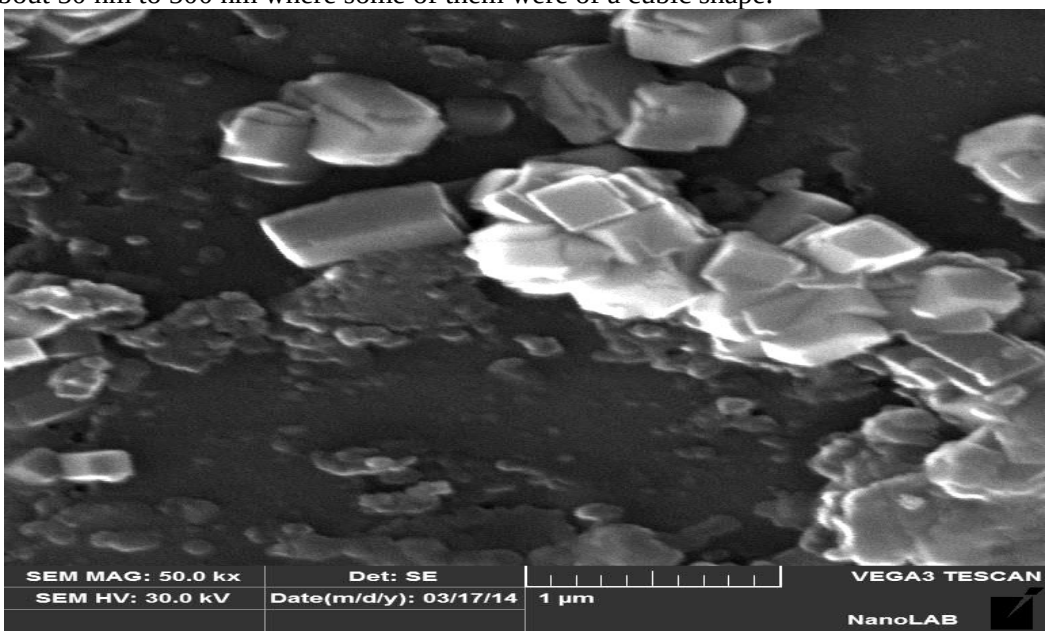

Figure 3-SEM image of SnO_2 thin film prepared at 300 ^{o}C

The TEM image for SnO_2 is shown in Figure-4. The TEM micrograph had shown the construction of well-defined SnO_2 as clusters which had diameters ranging from about 80nm to 120 nm.

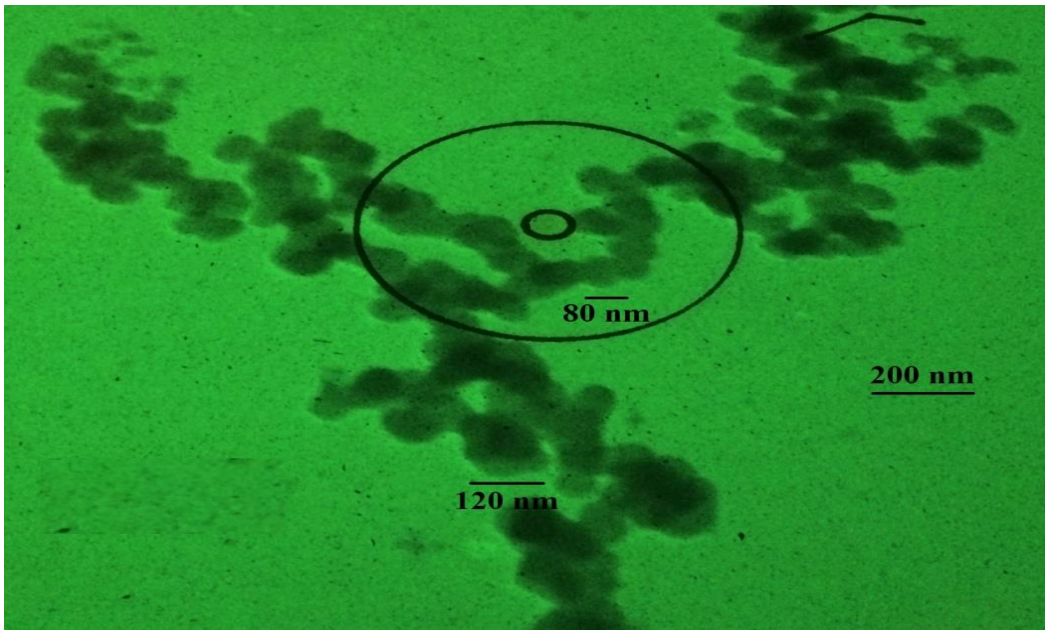

Figure 4-TEM images of SnO_2 nanoparticles prepared at 300 ^oC.

Atomic force micrographs allow us to get topographic information about the surface structure which represented by the surface relief. This technique along with special software offers digital images which allow a quantitative measurement of surface features, such as, roughness average and (RMS) which were equal to (0.703nm) and (0.882) respectively, as shown in Figure-5. The average grain size was equal to (82 nm).The ball shaped particles and the grains were higher homogenous and regular distribution.

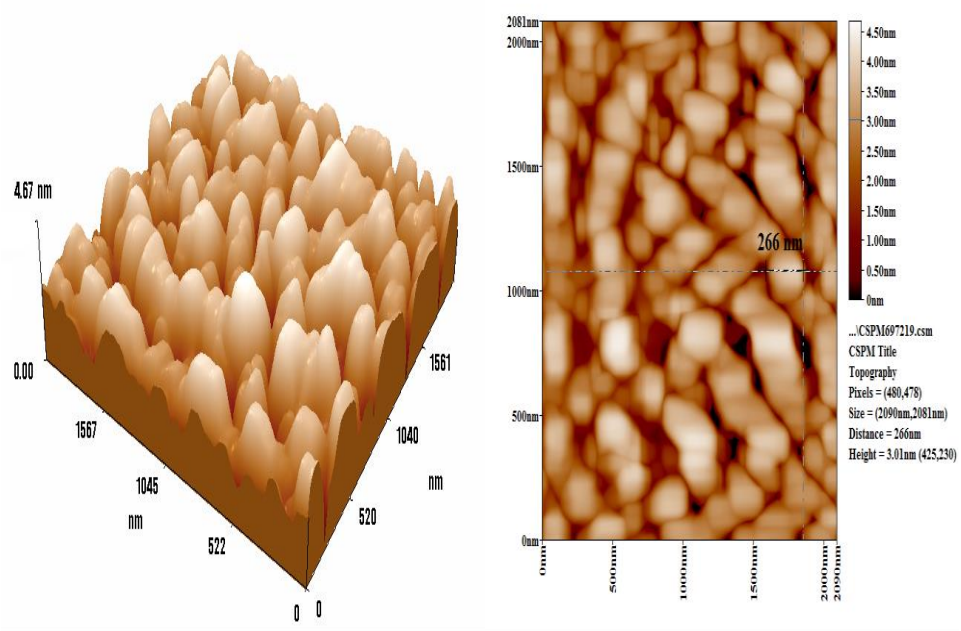

Figure 5-3D and 2D AFM images of SnO_2 thin film prepared at 300 ^oC.

Figure 6-shows the optical absorbance spectrum of SnO_2 films as a function of wavelength. This thin film had shown mid transparency (40 % -60 %) in the visible region- near infrared (380–1120) nm.

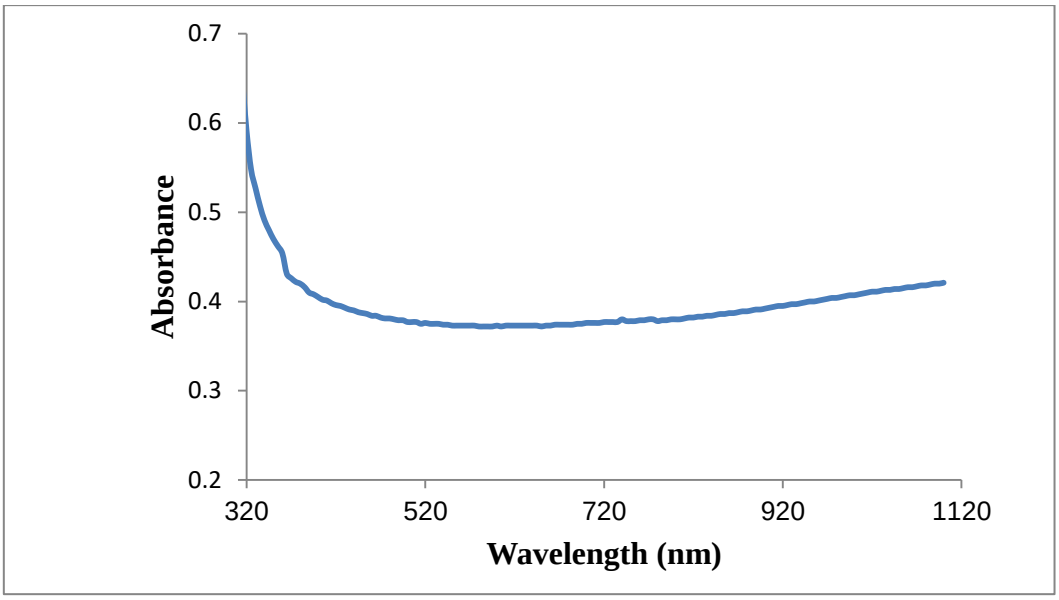

Figure 6-Optical Absorbance spectrum of SnO_2 thin film prepared at 300 °C.

By employing Tauc relationship, the absorption data can be used for the estimation of the band energy of SnO_2 thin film by plotting of $(\alpha h\nu)^2$ versus photon energy ($h\nu$). The extrapolation of the straight line to $(\alpha h\nu)^2=0$ gives the evaluation of the optical energy gap. Figure-7 Shows the $(\alpha h\nu)^2$ versus photon energy for SnO_2 film prepared at 300 °C oxidation temperature. The value of the optical band gap of SnO_2 film was measured to be around 3.58 eV, which depends on the oxidation temperature. The transition of electrons was found to be a direct transition type. These results agree with the results of Terrier et al.[16] and Patil et al. [17] and also were similar to other transparent conducting oxide thin films which have a wide band gap [18].

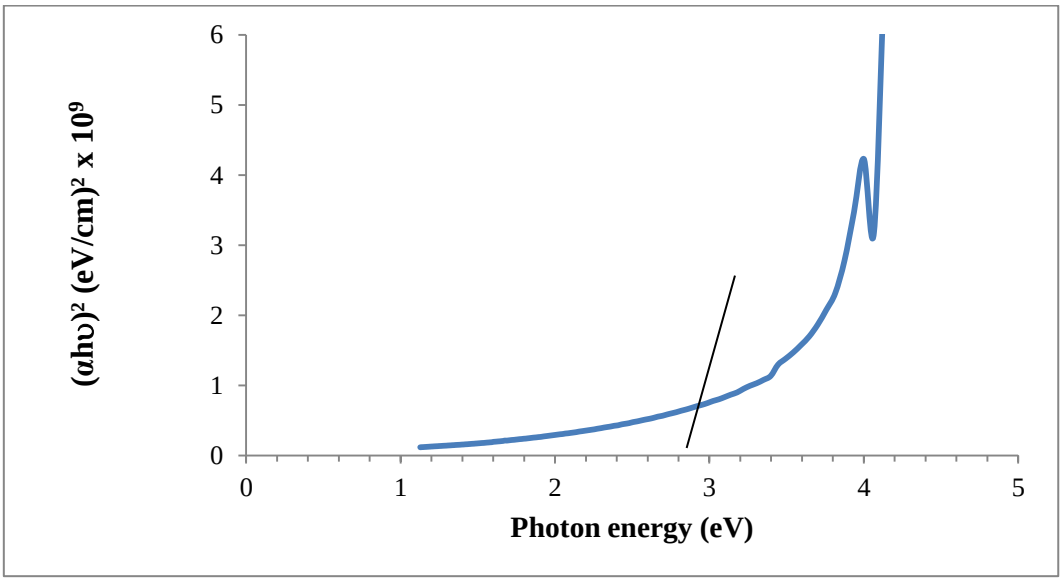

Figure7-$(\alpha h\nu)^2$ versus photon energy of SnO_2 film prepared at 300 °C.

Thin films specimens are examined for gas sensing using NO_2 at different operating temperatures. The sensitivity factor (S %) is calculating by equation **$(S=|(R_g-R_a) / R_a |*100\%)$** . Where, R_g and R_a the electrical resistance of the film in the presence of gas and air, respectively**,** Figure-8) shows the SnO_2 thin film mechanism of changing resistance with time duration to exposing to NO_2 gas, the resistance was allowed to stabilize without farther changing by stabilizing an operating temperature for 15 min. The variation of resistance was taken as R_a (Gas_{on}) without exposed to NO_2 gas. The changed resistance was taken as R_g (Gas_{off}) after exposing the film to the NO_2 gas, The oxidizing gas NO_2

reacts with film surface oxygen ions, the surface oxidation of film increases, and the number of free carriers was decreased, for this reason, the resistance increased with oxidant gases.

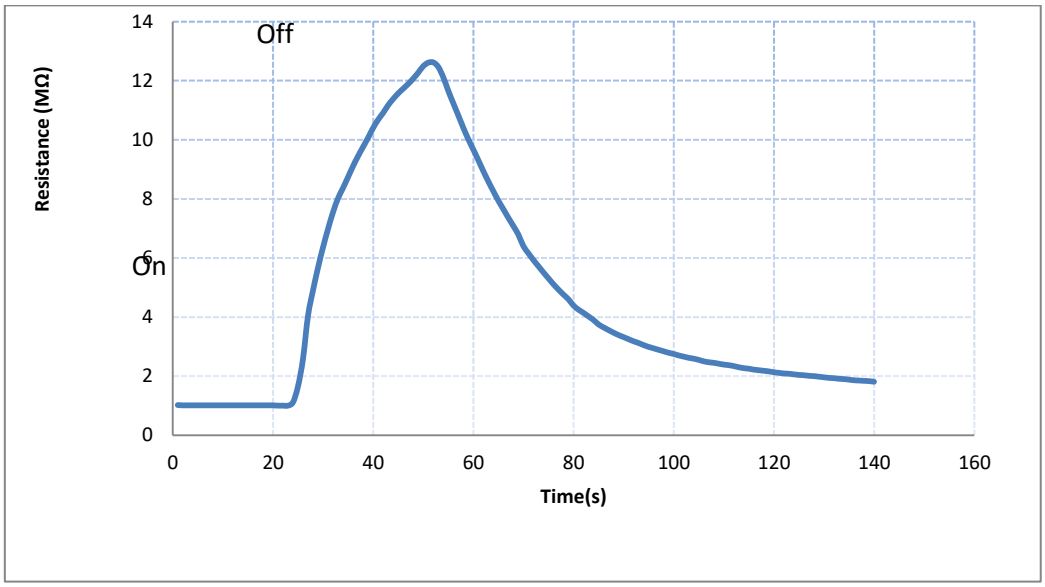

Figure 8-The variation of resistance with time for SnO_2 against NO_2 gas at operating temperature (200^{o}C).

The maximum value for sensitivity is observed to be shifted to higher operating temperatures as shown in Figure-9, The sensitivity was increasing with operating temperature up to 200 °C and the sensitivity decreased after that. Where the maximum gas sensitivity of SnO_2 is 1036 % at 200^{o}C. Because of increases in the SnO_2 molecular vibration and speed up gas diffusion when increasing operation (working) temperature, therefore the sensor sensitivity would be increased with increasing operating temperature through enhancement gas adsorption and the dissociation rate of the sensor's surface.

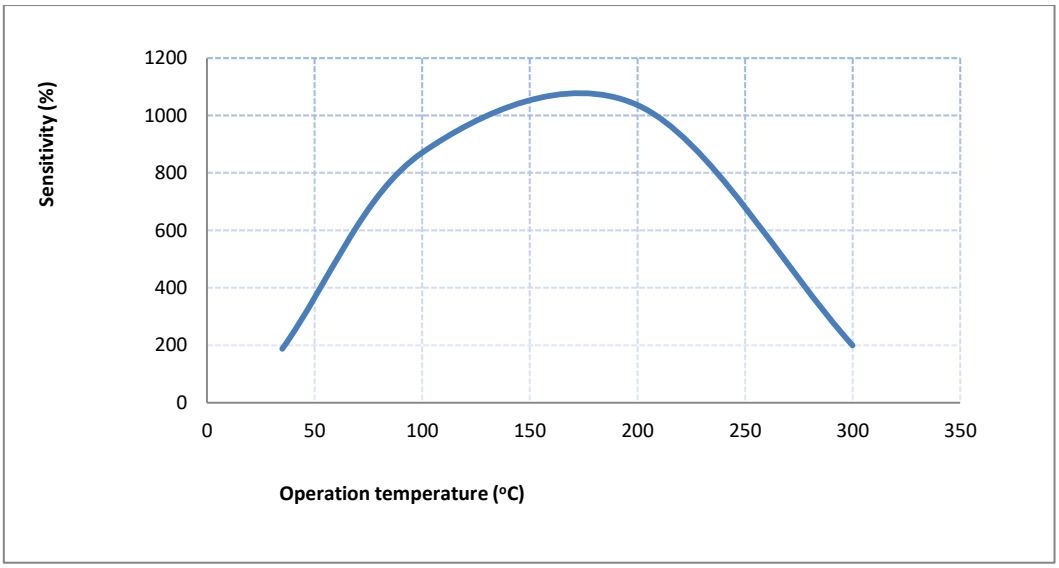

Figure 9-The sensitivity with working temperature for SnO_2 against NO_2 gas.

Figure-10 shows the response time and recovery time which are known as the times wanted for a sensor to reach 90 % of its whole response. The SnO_2 response and recovery times were successive tests Where response and recovery times decreased with increasing operating temperature.

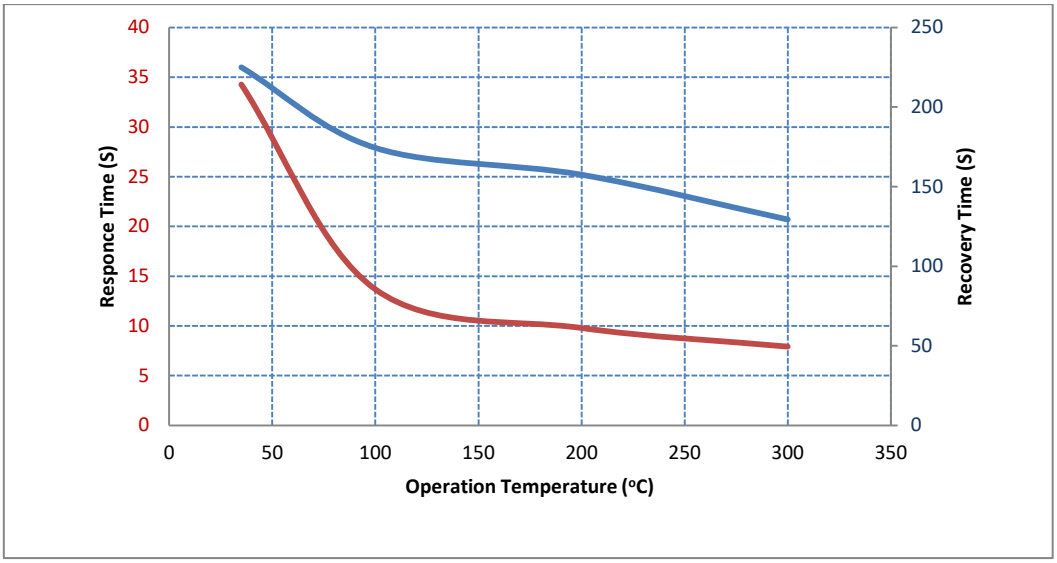

Figure 10-The response and recovery time with working temperature for SnO_2 against NO_2 gas.

4. Conclusions

This work had clearly demonstrated how SnO_2 thin films could be prepared by a simple and cheap method. The behavior of SnO_2 thin film as illustrated in the given graphs had shown that the films were having higher sensitivity and low response and recovery time which were indicative for NO_2 gas sensing device.The XRD patterns had revealed that SnO_2 semiconductor can be formed from a metallic material Sn by thermal oxidation at 300 ^oC temperature. SEM, TEM, and AFM have shown that nanoparticles average size exists and the surface was nanostructured.

Acknowledgment

I would like to thank Al-mustansiriyah University (www.uomustansiriyah.edu.iq) for their support in finishing this research.

References

1. Fang F., Futter J., Markwitz A. and Kennedy J. **2009** "UV and humidity sensing properties of ZnO nanorods prepared by the arc discharge method," *Nanotechnology*, **20**(24): 245502.
2. Fang F., Kennedy J., Futter J., Hopf T. , Markwitz A., Manikandan E. and Henshaw G. **2011** "Size-controlled synthesis and gas sensing application of tungsten oxide nanostructures produced by arc discharge," *Nanotechnology*, **22**(33): 335702.
3. Fang F., Kennedy J., Manikandan E. , Futter J. and Markwitz A. **2012** "Morphology and characterization of TiO2nanoparticles synthesized by arc discharge," *Chem. Phys. Lett.*, **521**: 86–90.
4. Kasinathan K., Kennedy J., Elayaperumal M., Henini M. and Malik M. **2016** "Photodegradation of organic pollutants RhB dye using UV simulated sunlight on ceria based TiO2 nanomaterials for antibacterial applications," *Sci. Rep.*, **6**(1): 38064.
5. Kaviyarasu K., Manikandan E., Kennedy J., Jayachandran M. and Maaza M. **2016** "Rice husks as a sustainable source of high quality nanostructured silica for high performance Li-ion battery requital by sol-gel method - a review," *Adv. Mater. Lett.*,**7**(9): 684–696.
6. Kaviyarasu K. , Manikandan E., Kennedy J. and Maaza M. **2016** "Synthesis and analytical applications of photoluminescent carbon nanosheet by exfoliation of graphite oxide without purification," *J. Mater. Sci. Mater. Electron.*, **27**(12): 13080–13085.
7. Kaviyarasu K., Ayeshamariam A., Manikandan E., Kennedy J., Ladchumananandasivam R. , Umbelino Gomes U., Jayachandran M. and Maaza M. **2016** "Solution processing of CuSe quantum dots: Photocatalytic activity under RhB for UV and visible-light solar irradiation," *Mater. Sci. Eng. B Solid-State Mater. Adv. Technol.*, **210**: 1–9.
8. Kaviyarasu K. , Manikandan E., Kennedy J. and Maaza M. **2015.** "A comparative study on the morphological features of highly ordered MgO:AgO nanocube arrays prepared via a hydrothermal method," *RSC Adv.*, **5**(100): 82421–82428.

9. Tagliente, M. A., Bello, V., Pellegrini, G., Mattei, G., Mazzoldi, P. and Massaro, M. **2009** "SnO2nanoparticles embedded in silica by ion implantation followed by thermal oxidation," *J. Appl. Phys.*, **106**(10).

10. Wang, X., Ren, P., Tian, H., Fan, H., Cai, C. and Liu, W. **2016.** "Enhanced gas sensing properties of SnO2: The role of the oxygen defects induced by quenching," *J. Alloys Compd.*, **669**: 29–37.

11. Nathera, A., Al-tememee, A., Mohammed, A., Hmeed, A., Fuad, A. and Ibrahim, T. **2014** "Crystalline Structure and Surface Morphology of Tin Oxide Films Grown by DC-Reactive Sputtering," **4**(2): 516–519.

12. Ayeshamariam, A., Sanjeeviraja, C. and Samy, R. P. **2013.** "Synthesis, structural and optical characterizations of SnO2 nanoparticles," *J. Photonics Spintron.*, **2**(2): 4.

13. Zhao, Y. and Zhang, J. **2008.** "Microstrain and grain-size analysis from diffraction peak width and graphical derivation of high-pressure thermomechanics," *J. Appl. Crystallogr.*, **41**(6): 1095–1108.

14. Pinheiro, M. A. L., Pineiz, T. F., de Morais, E. A., Scalvi, L. V. A., Saeki, M. J. and Cavalheiro, A. A. **2008.** "Schottky emission in nanoscopically crystallized Ce-doped SnO2 thin films deposited by sol-gel-dip-coating," *Thin Solid Films*, **517**(2): 976–981.

15. Chaki, S. H., Chaudhary, M. D. and Deshpande, M. P. **2014.** "Synthesis and characterization of different morphological SnS nanomaterials," *Adv. Nat. Sci. Nanosci. Nanotechnol.*, **5**(4).

16. Terrier, C., Chatelon J. P. and Roger, J. A. **1997.** "Electrical and optical properties of Sb:SnO2thin films obtained by the sol-gel method," *Thin Solid Films*, **295**(1–2): 95–100.

17. Patil, P., Kawar, R., Seth, T., Amalnerkar, D. and Chigare, P. **2003.** "Effect of substrate temperature on structural, electrical and optical properties of sprayed tin oxide (SnO2) thin films," *Ceram. Int.*, **29**(7): 725–734.

18. Kennedy, J., Murmu, P. P., Leveneur, J., Markwitz, A. and J. and Futter, J. **2016.** "Controlling preferred orientation and electrical conductivity of zinc oxide thin films by post growth annealing treatment," *Appl. Surf. Sci.*, **367**: 52–58.